Cheng et al., http://www.jcb.org/cgi/content/full/jcb.201501038/DC1

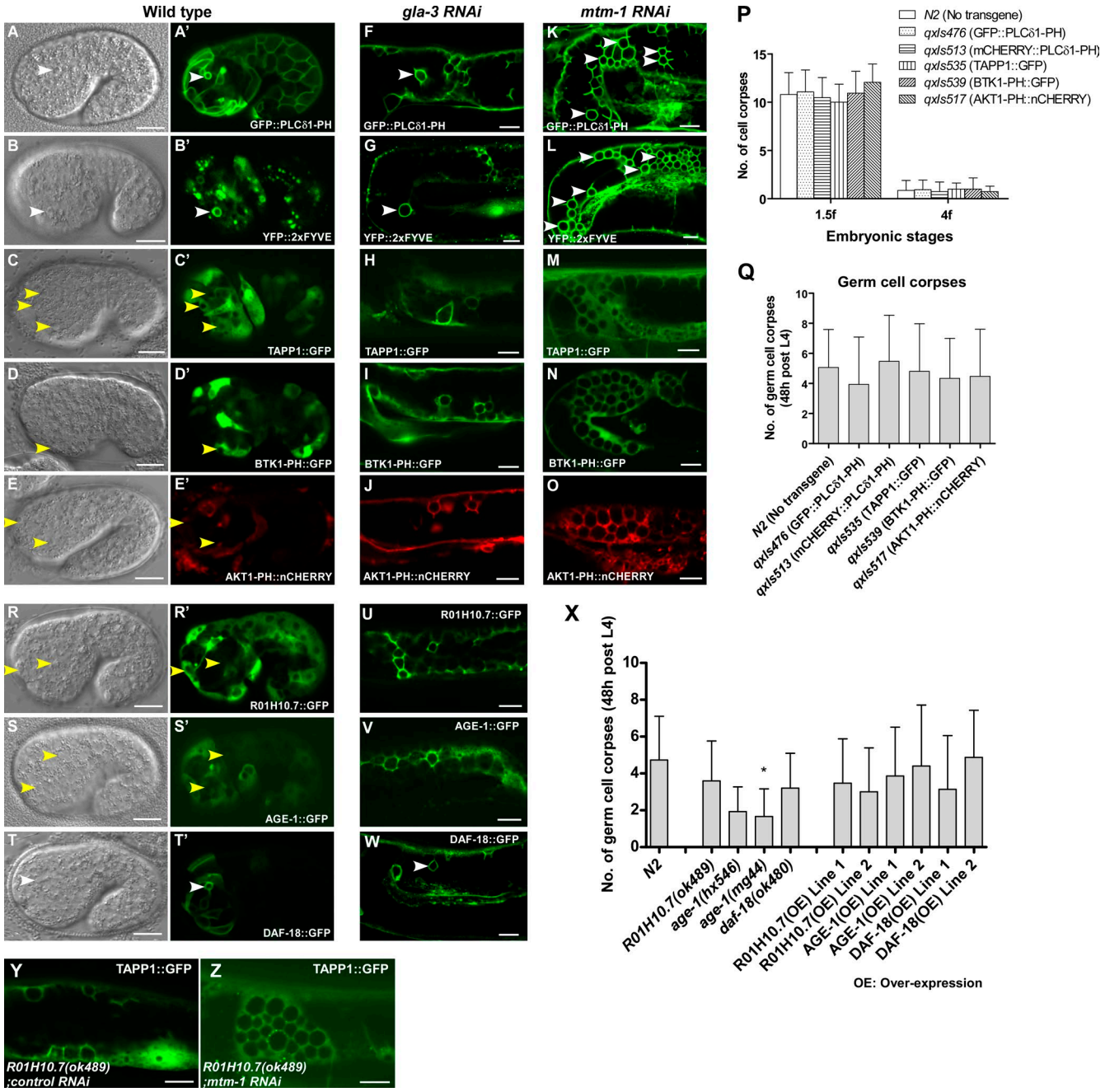

Figure S1. **PtdIns(3,4)P_2 and PtdIns(3,4,5)P_3 do not accumulate significantly on apoptotic cell–containing phagosomes.** (A–O) DIC and fluorescent images of wild-type embryos (A–E′) and the gonads in *gla-3RNAi* (F–J) or *mtm-1RNAi* (K–O) worms expressing GFP::PLCδ1-PH (A, A′, F, and K), YFP::2xFYVE (B, B′, G, and L), TAPP1::GFP (C, C′, H, and M), BTK1-PH::GFP (D, D′, I, and N), and AKT1-PH::nCHERRY (E, E′, J, and O). White and yellow arrowheads indicate labeled and nonlabeled cell corpses, respectively. (P and Q) Expression of PI sensors does not affect cell corpse clearance. Embryonic (P) and germ cell corpses (Q) are quantified in wild-type (*N2*) and reporter strains expressing biosensors of PIs. (R–W) DIC and fluorescent images of wild-type embryos (R–T′) or gonads (U–W) expressing R01H10.7::GFP (R, R′, and U), AGE-1::GFP (S, S′, and V), or DAF-18::GFP (T, T′, and W). The white and yellow arrowheads indicate labeled and nonlabeled cell corpses, respectively. In rare cases, DAF-18::GFP can be seen on the phagosome (arrowheads, T, T′, and W). (X) Quantification of germ cell corpses in the indicated strains at 48 h after L4/adult molt. (Y and Z) Fluorescent images of the gonads expressing TAPP1::GFP in *R01H10.7(ok489);controlRNAi* (Y) or *R01H10.7(ok489);mtm-1RNAi* worms (Z). No obvious phagosomal labeling was observed. (P, Q, and X) At least 15 animals were scored in each strain, and data are shown as mean ± SD. A two-way ANOVA (P) or one-way ANOVA with Tukey's post-test (Q and X) was performed to compare all the other datasets with that of the wild type (*N2*). No significant differences were found in P and Q, with P = 0.4288 and P = 0.7643, respectively. (X) *, P < 0.05. Other points had P > 0.05. Bars, 10 µm.

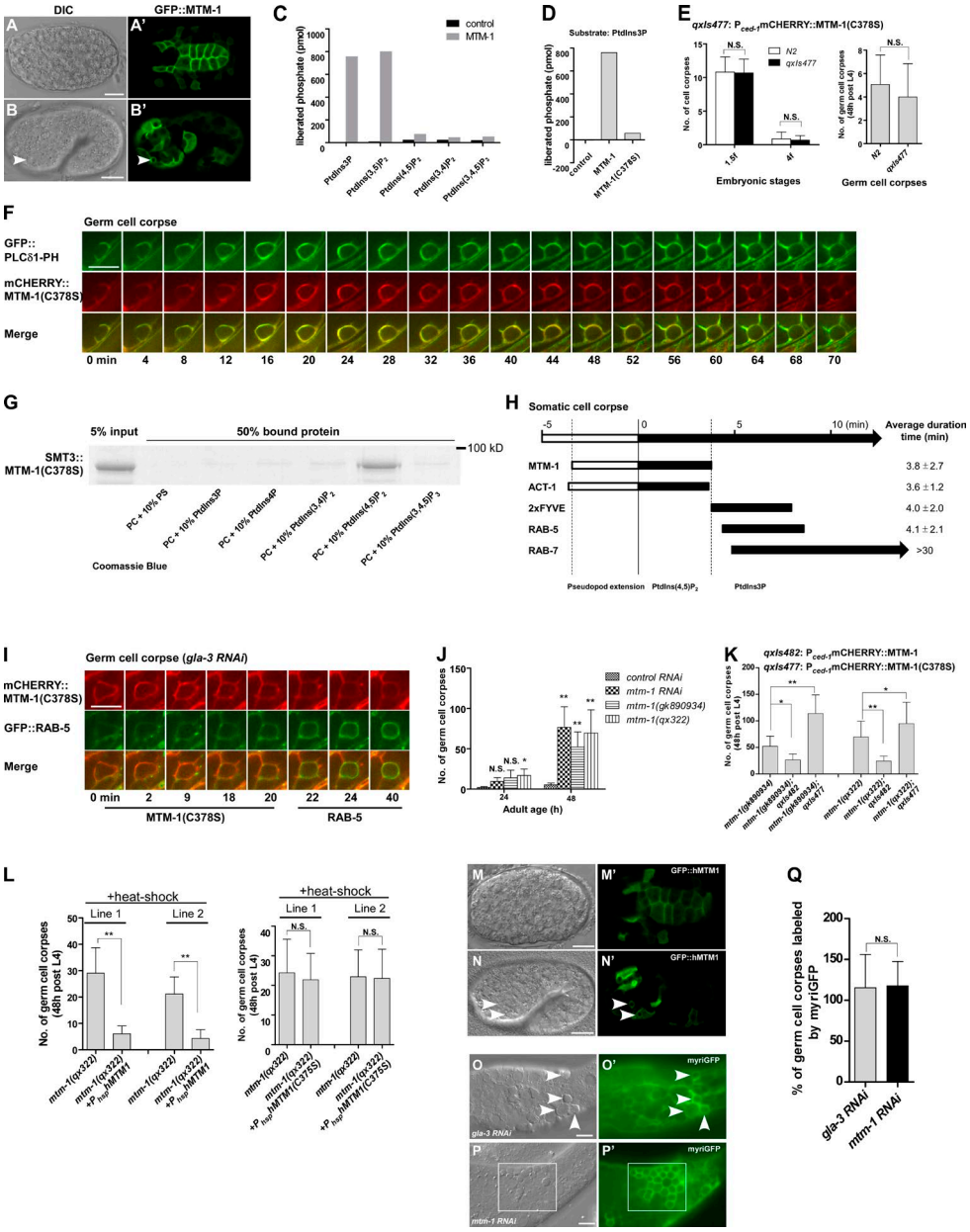

Figure S2. **MTM-1 acts at the PtdIns(4,5)P_2-positive stage to regulate apoptotic cell clearance.** (A–B′) DIC and fluorescent images of wild-type embryos expressing GFP::MTM-1. Arrowheads point to a cell corpse surrounded by GFP::MTM-1. (C and D) MTM-1 but not MTM-1(C378S) displays phosphatase activity toward PtdIns3P and PtdIns(3,5)P_2. Triplicate samples were measured to get the mean value of liberated phosphate (picomoles). (E) Expression of mCHERRY::MTM-1(C378) does not affect apoptotic cell removal. Embryonic (left) and germ cell corpses (right) were scored in wild-type (*N2*) and *qxIs477* worms that express mCHERRY::MTM-1(C378S) from a genome-integrated array. At least 15 animals were scored. Unpaired *t* tests were performed. (F) Time-lapse images of a germ cell corpse in a wild-type worm expressing GFP::PLCδ1-PH and mCHERRY::MTM-1(C378S). PLCδ1-PH and MTM-1 display identical phagosomal dynamics. Images in 20–25 z series were captured in the time-lapse recording, and representative images are shown. (G) MTM-1(C378S) binds to liposomes containing 10% PtdIns(4,5)P_2 but not other PIs in a liposome flotation assay. (H) Time-course analysis of phagosomal recruitment of MTM-1, ACT-1, 2xFYVE, RAB-5, and RAB-7 during phagocytosis of embryonic cell corpses. Time-lapse images of wild-type embryos coexpressing mCHERRY::MTM-1(C378S) and GFP::ACT-1, YFP::2xFYVE, GFP::RAB-5, or GFP::RAB-7 were collected and analyzed. The time point when cell corpses were surrounded by MTM-1(C378S) is defined as "0 min." White bars indicate pseudopod extension, and black bars designate the sequential appearance and duration of phagosomal markers. At least 10 cell corpses from three animals were followed in each strain to determine the mean duration of each marker. (I) Time-lapse images of a germ cell corpse in a *gla-3RNAi* animal coexpressing mCHERRY::MTM-1(C378S) and GFP::RAB-5. MTM-1 release precedes RAB-5 appearance on the phagosome. (J) Loss of MTM-1 causes accumulation of germ cell corpses. (K) The germ cell corpse phenotype of *mtm-1* mutants can be rescued by expression of MTM-1 but not MTM-1(C378S). (L) The germ cell corpse phenotype of *mtm-1(qx322)* can be rescued by expression of human MTM1 but not hMTM1(C375S). Two independent transgenic lines were examined. (M–N′) DIC and fluorescent images of wild-type embryos expressing GFP::hMTM1. hMTM-1 is observed on plasma membranes and phagosomes (arrowheads). (O–P′) DIC and fluorescent images of the gonads in *gla-3RNAi* (O and O′) or *mtm-1RNAi* (P and P′) animals expressing myriGFP, which labels plasma membranes. White arrowheads and boxes indicate germ cell corpses labeled by myriGFP. Quantification is shown in Q. (J–L and Q) Germ cell corpses were quantified in the indicated strains at 24 or 48 h after L4/adult molt. At least 15 animals were scored in each strain. In J–L, a two-way ANOVA with the Bonferroni post-test was performed to compare all the other datasets with that of *control RNAi* (J) or datasets linked by lines (K and L). *, $P < 0.05$; **, $P < 0.001$. In Q, the unpaired *t* test was performed. Data are show as mean ± SD. Bars, 10 µm.

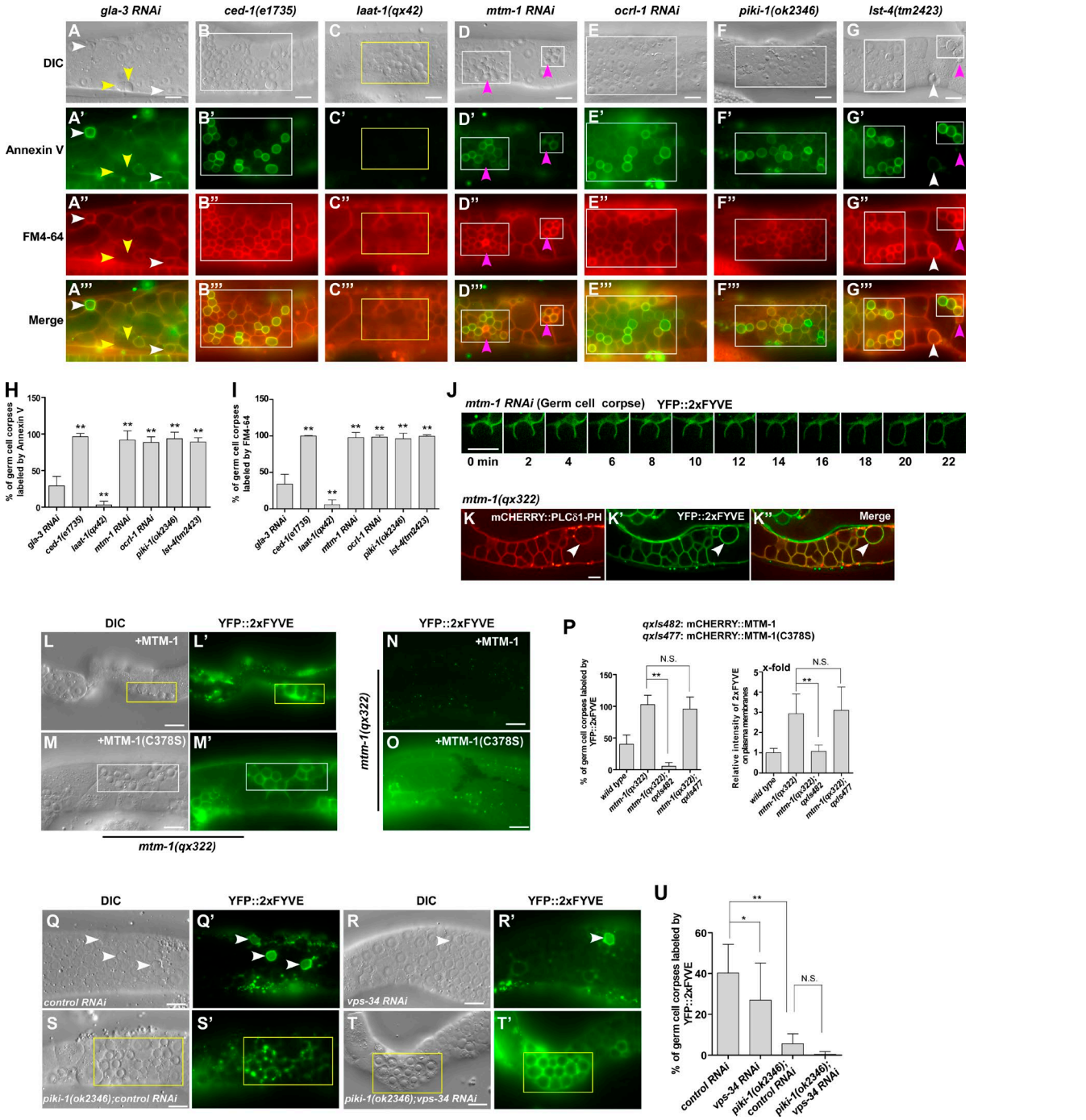

Figure S3. **MTM-1 regulates PtdIns3P levels on plasma membranes, extending pseudopods, and phagosomes.** (A–G''') DIC and fluorescent images of the gonads in the indicated strains stained by both Alexa Fluor 488–conjugated Annexin V and FM4-64 are shown. White boxes and arrowheads point to cell corpses that are labeled by both FM4-64 and Annexin V, and yellow ones indicate unlabeled cell corpses. The fluorescence intensity of Annexin V conjugates varied on different apoptotic cells. In rare cases, FM4-64–positive but Annexin V–negative cell corpses were observed (pink arrowheads). (H and I) The percentage of cell corpses labeled by Annexin V (H) and FM4-64 (I) was quantified in the indicated strains at 36 h after L4/adult molt. (J) Time-lapse images of a germ cell corpse in an *mtm-1RNAi* animal expressing YFP::2xFYVE. PtdIns3P accumulates on extending pseudopods in *mtm-1RNAi*. At least 10 cell corpses from three animals were followed. Images in 20–25 z series were collected, and representative images are shown. (K–K'') Fluorescent images of the gonad in an *mtm-1(qx322)* mutant coexpressing mCHERRY::PLCδ1-PH and YFP::2xFYVE. Loss of *mtm-1* causes PtdIns3P accumulation on the PtdIns(4,5)P_2-positive phagosome (arrowheads). (L–O) DIC and fluorescent images of the gonads in *mtm-1(qx322)* mutants coexpressing YFP::2xFYVE and MTM-1 (L, L', and N) or MTM-1(C378S) (M, M', and O) in the middle (L–M') or top (N and O) focal plane. The white and yellow boxes indicate YFP-positive and -negative germ cell corpses, respectively. (P) Quantification of phagosomal labeling (left) and relative intensity of YFP::2xFYVE on plasma membranes (right) in *mtm-1(qx322)* expressing MTM-1 or MTM-1(C378S). Expression of MTM-1 but not MTM-1(C378S) significantly reduces PtdIns3P accumulation on phagosomes and plasma membranes in *mtm-1(qx322)*. (Q–T') DIC and fluorescent images of the gonads in the indicated strains expressing YFP::2xFYVE. White arrowheads indicate YFP-positive germ cell corpses, and yellow boxes indicate nonlabeled corpses. Quantification is shown in U. (H, I, P, and U) At least 10 (H and I) or 15 animals (P and U) were scored in each strain, and data are shown as mean ± SD. A one-way ANOVA with Tukey's post-test was performed to compare all the other datasets with that of *gla-3RNAi* or datasets that are linked by lines. *, $P < 0.05$; **, $P < 0.0001$. Bars, 10 µm.

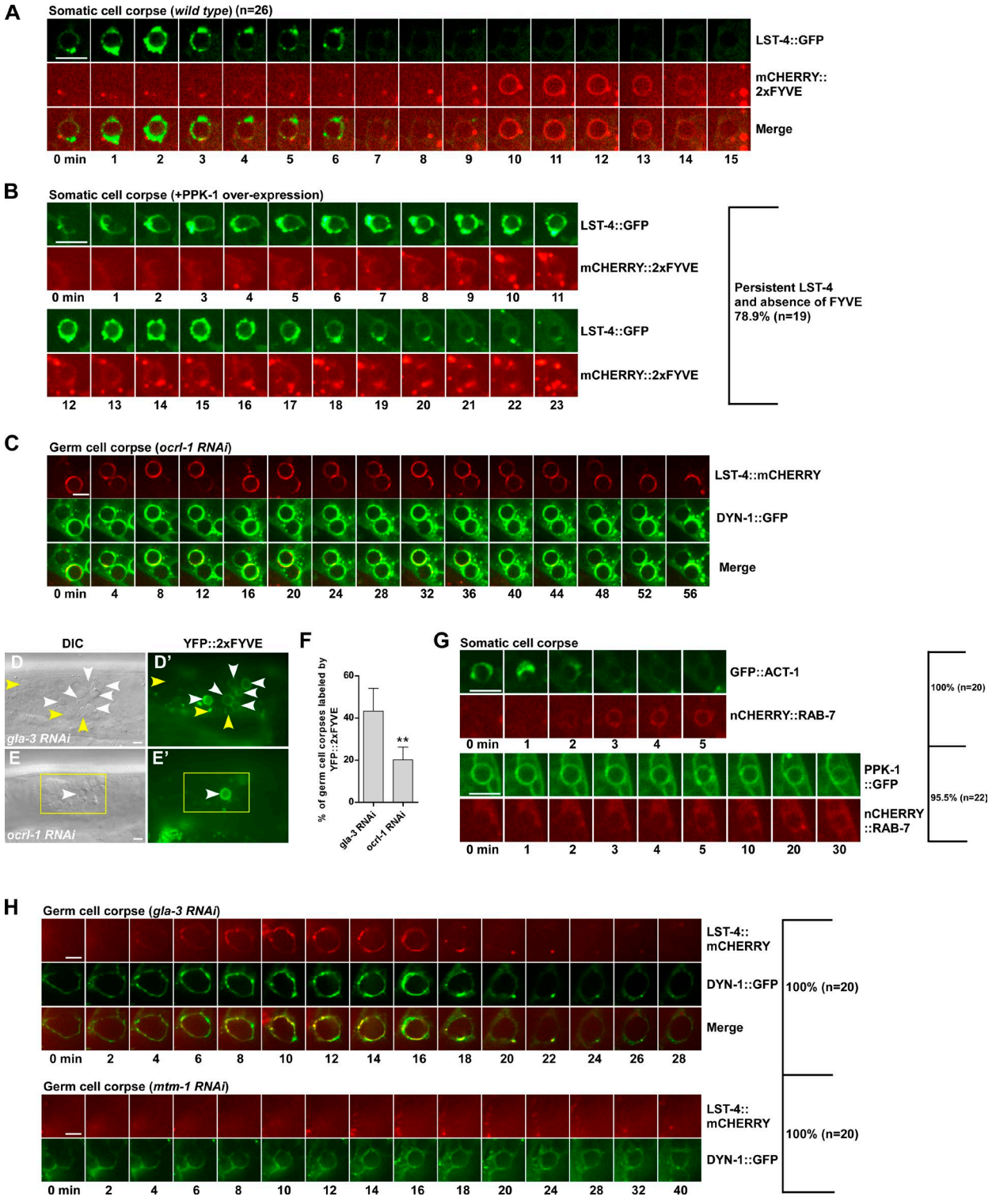

Figure S4. **Phagosomal association of LST-4 is regulated by PtdIns(4,5)P_2, MTM-1, and PIKI-1.** (A) Time-lapse images of a cell corpse in a wild-type embryo coexpressing LST-4::GFP and mCHERRY::2xFYVE. (B) Time-lapse images of a cell corpse in a wild-type embryo coexpressing PPK-1, LST-4::GFP, and mCHERRY::2xFYVE. (C) Time-lapse images of germ cell corpses in an *ocrl-1RNAi* animal coexpressing LST-4::mCHERRY and DYN-1::GFP. Loss of *ocrl-1* causes sustained LST-4 and DYN-1 on phagosomes. (D–E') DIC and fluorescent images of the gonads in *gla-3RNAi* or *ocrl-1RNAi* animals expressing YFP::2xFYVE. White arrowheads indicate germ cell corpses labeled by phagosomal markers, and yellow arrowheads and boxes indicate unlabeled corpses. Quantification is shown in F. At least 15 animals were scored in each strain, and data are shown as mean ± SD. The unpaired *t* test was performed. **, $P < 0.0001$. (G) Time-lapse images of cell corpses in wild-type embryos coexpressing nCHERRY::RAB-7 and GFP::ACT-1 or PPK-1::GFP. The time point when the cell corpse is surrounded by GFP::ACT-1 or PPK-1::GFP is defined as "0 min." Expression of PPK-1::GFP blocks recruitment of RAB-7 to the phagosome. (H) Time-lapse images of germ cell corpses in *gla-3RNAi* or *mtm-1RNAi* animals coexpressing LST-4::mCHERRY and DYN-1::GFP. (B, G, and H) The percentage of phagosomes with the representative pattern was quantified and is shown at the right. "n" indicates the number of phagosomes that were followed and quantified. In all time-lapse recordings, images in 20–25 z series were captured, and representative images are shown. Bars, 5 µm.

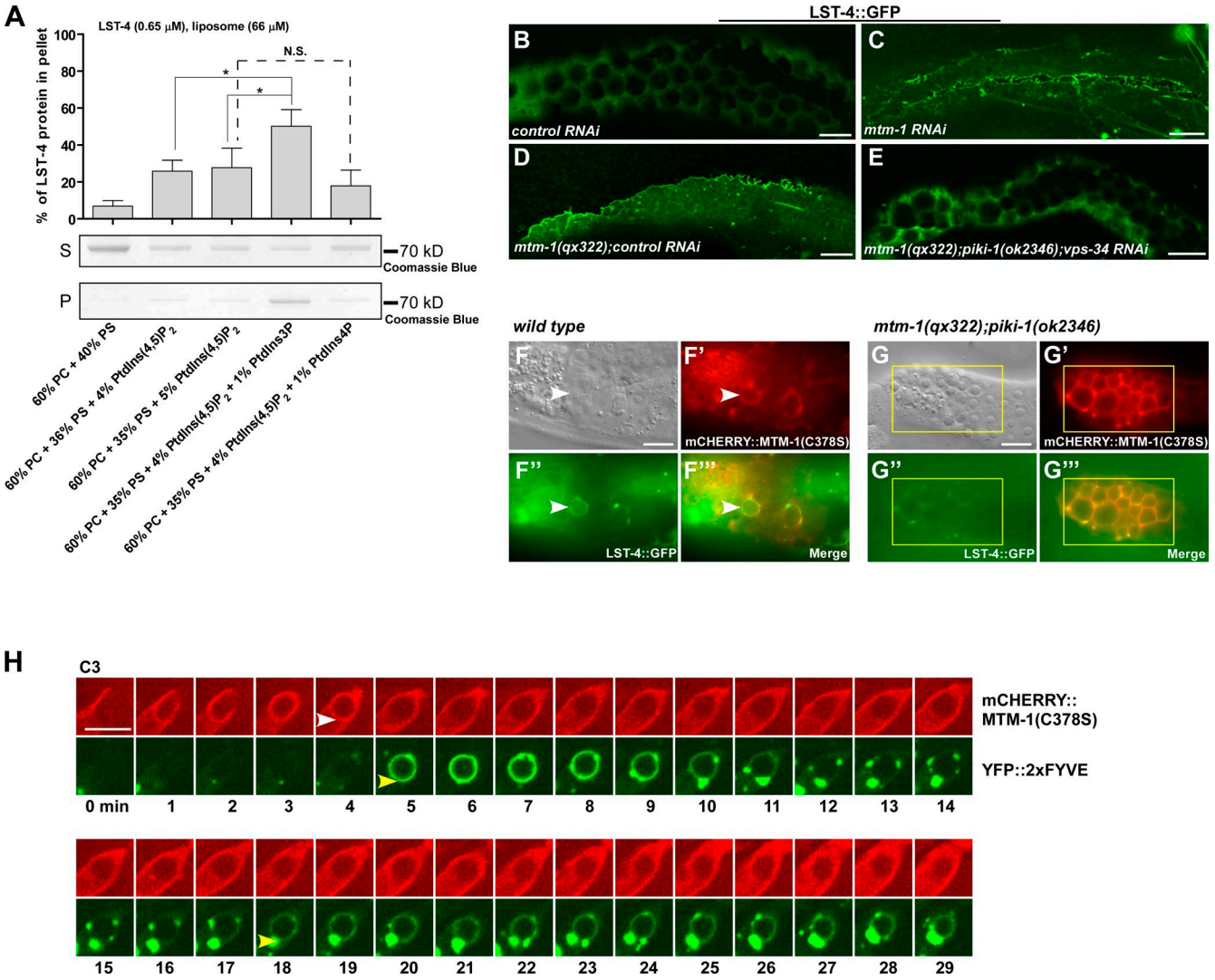

Figure S5. **PtdIns3P enhances LST-4 binding to PtdIns(4,5)P_2 liposomes.** (A) Binding of His-tagged LST-4 to the indicated PC/PS liposomes was detected by Coomassie blue staining. The lipid–protein complex is recovered in the pellet (P) but not the supernatant (S). The final concentration of LST-4 and liposomes used in each experiment is indicated. Five independent experiments were performed, and data are shown as mean ± SD. Data were compared by a one-way ANOVA with Tukey's post-test. *, $P < 0.05$. (B–E) Fluorescent images of gonadal sheath cells in the indicated strains expressing LST-4::GFP driven by heat-shock promoters were captured on the top focal plane to show the cell surface labeling. Loss of *mtm-1* causes accumulation of LST-4 on the cell surface, which is suppressed by inactivation of PIKI-1 and VPS-34. At least 15 animals were examined in each strain, and representative images are shown. (F–G‴) DIC and fluorescent images of gonadal sheath cells in wild type (F–F‴) and *mtm-1(qx322);piki-1(ok2346)* (G–G‴) coexpressing mCHERRY::MTM-1(C378S) and LST-4::GFP. LST-4::GFP was observed on phagosomes in wild type (white arrowheads) but not an *mtm-1(lf);piki-1(lf)* double mutant (yellow boxes). (H) Time-lapse images of C3 in a wild-type embryo expressing both mCHERRY::MTM-1(C378S) and YFP::2xFYVE. "0 min" represents the time point when MTM-1(C378S) was initially detected around the cell corpse. The white arrowhead indicates mCHERRY::MTM-1(C378S) on the C3 phagosome before its disappearance. The yellow arrowheads indicate the initial and reappearance of YFP::2xFYVE on the C3 phagosome. mCHERRY::MTM-1(C378) disappearance coincides with YFP::2xFYVE enrichment on the C3 phagosome, and no reappearance of MTM-1 is observed. At least 10 C1, C2, or C3 phagosomes were followed at multiple z positions, and similar dynamics were observed. Representative images of C3 are shown. Bars: (H) 5 μm; (B–G) 10 μm.

Table S1. **LST-4 acts in the same pathway with MTM-1 and PIKI-1 to regulate apoptotic cell clearance**

Genotype	No. of germ cell corpses	P-value
control RNAi	0.9 ± 0.8	
vps-34 RNAi	3.1 ± 1.7	
piki-1(ok2346);control RNAi	11.7 ± 4.4	
piki-1(ok2346);vps-34 RNAi	18.6 ± 5.9	0.0015[a]
lst-4(tm2423);control RNAi	16.7 ± 3.0	
mtm-1(qx322);control RNAi	19.3 ± 4.5	0.053[b]
mtm-1;lst-4;control RNAi	18.7 ± 5.5	0.201[c]
lst-4(tm2423);control RNAi	16.7 ± 3.0	
piki-1(ok2346);vps-34 RNAi	18.6 ± 5.9	0.242[d]
lst-4(tm2423);vps-34 RNAi	11.8 ± 3.4	
lst-4;piki-1;control RNAi	17.3 ± 6.7	
lst-4;piki-1;vps-34 RNAi	18.1 ± 6.7	0.439[e]
piki-1(ok2346);vps-34 RNAi	18.6 ± 5.9	
mtm-1(qx322);control RNAi	19.3 ± 4.5	0.714[f]
mtm-1(qx322);vps-34 RNAi	25.7 ± 9.8	
mtm-1;piki-1;control RNAi	19.4 ± 6.2	
mtm-1;piki-1;vps-34 RNAi	23.1 ± 4.6	0.032[g]

Germ cell corpses in one gonad arm were quantified in the indicated strains at 24 h after L4/adult molt. At least 15 animals were scored in each strain, and data are shown as mean ± SD. Unpaired *t* tests were performed between the two experimental groups as follows.
[a]*piki-1(ok2346);controlRNAi* was compared with *piki-1(ok2346);vps-34RNAi*.
[b]*lst-4(tm2423);controlRNAi* was compared with *mtm-1(qx322);controlRNAi*.
[c]*lst-4(tm2423);controlRNAi* was compared with *mtm-1;lst-4;controlRNAi*.
[d]*lst-4(tm2423);controlRNAi* was compared with *piki-1(ok2346);vps-34RNAi*.
[e]*lst-4(tm2423);controlRNAi* was compared with *lst-4;piki-1;vps-34RNAi*.
[f]*piki-1(ok2346); vps-34RNAi* was compared with *mtm-1(qx322);controlRNAi*.
[g]*piki-1(ok2346); vps-34RNAi* was compared with *mtm-1;piki-1;vps-34RNAi*.

Table S2. **Primers used for plasmid construction**

Primer	Sequences (5′ to 3′)
PXL248	GCGGTACCATGGACTCGGGCCGGGACTTCC
PZHW42	AAGGTACCTTAGATGTTGAGCTCCTTCAGGAAG
PHBW40	GCGGTACCATGGCTTCTCGGTCCACAAC
PRM5	GCGGTACCTCAAGCGACAGGTGTGTC
PSYC401	GCGGTACCAGCGACAGGTGTGTCACCAC
PSYC545	GCGGTACCATGCCTTATGTGGATCGTCAG
PSYC546	GCGGTACCCACGTCACTGACCGGAAGGC
PSYC549	GCGGTACCATGGCCGCAGTGATTCTGGAG
PSYC550	GCGGTACCAGGTTTTAAGCTTCCATTCCTG
PPFG370	CTAGCTAGCATGAGCGACGTGGCTATTGTG
PXL297	CCGCTAGCGGCCCGGTCCTCGGAGAACAC
PWZ294	GCGGTACCATGAAATTACAGATTGATGCCGACCG
PWZ296	GCGGTACCCTATTTCTGGGAATCAGTGAAGCACG
PBL217	GCGGTACCATGAGCGACGATGAAGAGCTCCAACTAGCC
PBL218	CGGGTACCTTAGACACATTTTTCACAGTTGAACCATCC
PSYC521	GCCCCGGGATGCGGGCCGCAGGCCCGAATAC
PSYC522	GCGCTAGCACTGGCGACACCCTGCGAGTAG
PSYC501	GCCCCGGGATGTCTATGGGACGAAGCCCCT
PSYC502	GGGCTAGCGTAGTGTTTGACTGCGTGGAAG
PXL353	GCGGTACCATGGTTACTCCTCCTCCAGATG
PXL354	GCGGTACCCAAATAAATAGCTTGATC
PWZ386	CGGGTACCATGGCTTCTGCATCAACTTC
PWZ385	GCGGTACCTCAGAAGTGAGTTTGCACATGG
PWZ445	AGAGTTCAGTGCTTGTGCATTCCAGTGACGGATGGGACAGGACTG
PWZ446	CAGTCCTGTCCCATCCGTCACTGGAATGCACAAGCACTGAACTCT
PXLG1	GCGGATCCCATGGACTCGGGCCGGGA
PXLG2	GCCTCGAGGATGTTGAGCTCCTTCAGG
PSYC450	GGAATTCCATATGATGGCTCAGGTGAAAGCCGAG
PSYC452	GCCTCGAGATCATATCTAGCGGCTAATG
PWDL108	CGACTAGTATGGATGACAGAGGGAACAATAGTG
PWZ706	CGAAGCTTGGCGGTCAATTTTTGAGCAGC
PQL148	CAATCAGTATTGATTCATAGTTCTGATGGTTGGGATCGAAC
PQL149	GTTCGATCCCAACCATCAGAACTATGAATCAATACTGATTG
PSYC609	GCGCTAGCATGTCGGACTCAGAAGTCAATC
PSYC610	GCGGATCCCGGCTGCCGCGCGGCACCAGACCAATCTGTTCTCTGTGAGCC
PSYC602	GCAAGCTTATGGATGACAGAGGGAACAA
PSYC405	GCCTCGAGGGCGGTCAATTTTTGAGCAG
PSYC443	GCGGTACCCTACTTGTCATCGTCATCCTTGTAGTCGGCGGTCAATTTTTGAGCAG
PWK73	CATTAGCATATGTCCCCTATACTAGGTTATTG
PWK70	GCGCGGCCGCTCACTTGTCATCGTCATCCTTGTAGTCATCCGATTTTGGAGGATGG
PWZ215	CGGGTACCATGGATGACAGAGGGAACAATAGTG
PHWD377	GCGGTACCATGGCTCAGGTGAAAGCCGAGTA
PHWD375	GCGGTACCTCAATCATATCTAGCGGCTAATGA
PSYC645	GCGGTACCTCATCCTCGATCAGGTCCACCGTG
PSYC640	GCGGTACCCCATCACAGAATGATGATT

Table S3. **Double-stranded RNAs for RNAi experiment**

Gene	Corresponding DNA sequence of the double-stranded RNAs (5′- to -3′)	Location
gla-3	TCATTACCATGGAACTGGAAATCGTTTATCAAATTTCATGCCAGGACGTCATCGTCCCCCACATCAACATCCAATCCATCATCATCATCAGT CACAACATCAGCTACACCAGCATCAGCAATATCTGCATCATGCTGCTCAGCAATACCGTTATTCGCATCAACAGGGACCTCAACATCCGTTT GCGGCTCTTCTCTCACCACCGGAGATCTCGGAGTCCTTGCTCCCACCTGATGACTCGTTTTCGATTTGGCTCGAGCCGAAGCCGAAAAAACA GTCCGGAGCCATGACACGAACTCGCGGAGCTGCGACGATCAACGAATCGAGTTCTGCGGCAAGTCTGCTCACAAAAATGGATGCTCTTCGAT CAGACAAGTATCCAATTACAGACGAGGAAATGATGATGGCTAATGATTTTGTGAGACAAGGCGATCGAGATGGTATGTTTATTGGTTAATTT ACTCGAAAAATTTCTATAAAAATTTATAGTTCTGAATATCCATCAATTTCAGATAAACTAAGCTCCAGCGAAAGCTCAAGTCCTGTCGTGAT GTCTTTGATGGAACTATTGAGCAACGAGAATCTGCTCGATCAAGTAGCAACCGAAAAACCAAAGTGTTCTATGTTCGATTTTGATACTCTAA AAATCGCCGAAACTCTCAAGGAGCCACTGCAATCTTCCGAATGTTCAACTACAACATCAAGCAAGATGACCTGCTCTCCAATGTTCTTTTTC GTAGATGAAAAGACACCAAACTACGGTAAAATTTTTTTTAGTATTTGAGTAGAACCTCCAATATATCGGCTATTTTTTAGACGGCTCAGGAT CGAAAAGCCTTTTCACTCCGTCATCATCGGCCGGCCAGACGCCTTCATTCCTGGAACCTTGCGATTTTTTTGCAGCCACCGGATCGTGCCCC TTCGGTGACGCCTGTCATCAGAGTCACTCGATTTAGGAGGACCAGCGATGATTTTAAAGCCCATTATTGTAATCATTTTCTCATTTCTCACC CAATTCAGT	T02E1, 12,950–1,3970 nt
mtm-1	AAAGGAAATTTTCAGCCAATGTTCGCCTCTGTACATGCAGCAGAAACACCTAGACTTATGAAAGATGGTTGGAAAATTTATTCAGCTGAAAA AGAATATGAACGCCTTGGAATCCCGAATTCACGTCTTTGGAAAGAAGTGGACATTAATAAAGACTATAAATTTAGCGAAACTTATCCAAGAA CTGTAGGTTAATGATGGTTTTCTTTTTTAAAAATAATTTTATTTCAGTTTGTAATTCCGACAGTATCTTGGGAGGAAGGAAAACCATTTGTA AAGAAGCTCGGCGAGTTTAGAAGCAAAGAAAGAATTCCCGTGTTGAGTTGGATTAATCAGACAACTTTAGCTTCAATTTCACGATGCTCACA GCCAATGACTGGAATTTCTGGAAAAAGAAGTGCTGAGGACGAGCGGTAGGTTTTATTTTTATTTTTAATGATAATAAAAAATAATCGGAATA TTAATATTCTAATATGCTGAAATGTCACAAAAGAAAAACGAAAAAAAATATTTGGAAAATCGTTTATTAAGATATATTTTTTAAAGCATTCA ATTTTTCAACAAAAAATTATATTTTTCAGACATCTCACGAACATTATGAATGCCAATGCTAATTGTCGTGAACTTCTGATCCTTGATGCAAG ACCAGCAGTCAATGCAAAACTTAATAAGGCAAAAGGTGGAGGTTATGAAGAGAATTATGTCAATGCTCCTCTAACATTCCTCAATATTCACA ATATTCACGTTGTTCGGGATTCATTAAAACGATTGCTAGCCGCGCTGATTCCACGTGTCGACGAGAAGGGATACTACAAAGCGTTAGACGAA TCGAAATGGCTCAATCATGTTCAGAGCATTTTGGAAGGAGCAGTAAAAGCTGTCTTCAATGTTGACACTGAAAAACAATCAGTATTGATTCA TTGTTCTGATGGTTGGGATCGAACTGCACAGCTGACGTCGTTGGCAATGATTCAACTCGACTCCTATTACCGTACAATTGAAGGATTTATCG TTTTGATTGAGAAGGAATGGTGTAGCTTTGGTCATAAATTTGGAGAGAGAATCGGTTCGTTTTTGATAGATTTTAAAAATCATGCAATTAAA GTTGCAGTAGCGTGAATGAGGATTTTGCTTTTTTTAAAAATCCATTCAGAAAATTTTTAAAAAAATCAAAAAAATTGCGAAAAAAAAATCCAA CTTAAAAAACTAGATTTTTCAGTTCTGGCGAAGTTCCCAGTTCTCATCTTGGGGAAAATTCAAACAGGAAACTTACTAGGGAACACGATAAC TATAAGTTATACTTATAGTTATCGTGTTCCCTAGTTAGTCAAAATTGATAAATCGAATTTTTTAAAATTTGAATTTTTCATCCGTTCGCAAT TTTATTTCGTTTTTCTGTTGTGGTATTTCTGAATTTGAGAAAAATTTGGAATTTTTTGAAGCTAACAACTATAAAAAATATTATTTGAGAAC CAAAAATCTTTGATTTTATACTTTCCGTTCAGGTCACGGCGACGATAACTACAGCGATGGAGAACGATCTCCCGTATTTGTTCAATTCTGTG ACTGCCTATGGCAAATTATGCGACAATTTCCATGGGCATTTGAATTTACACAAGAACTGCTAATTTGTATGCTCGATGAGCTCTACGCTTGC AGATATGGAACATTTTTGTACAATTCCGAAAAAATCCGGCTGAAGGATAAGGTTGTTTTCATGAAGATTTTTTCAATTTTTTTTTTTTCAAC TTTTCAGAAATGCGATGAAACGACGATATCGTTCTGGTCCTATGTTTTGGAAAATAAAAAGAAATTCAGAAATCCAATGTTTAAGCATGGAA GTTAGTTTTCTGTTAAACTAATATTAAATCTCAAAATTTTAACTTTCAGAATCCAATAAAGTGATAAACGTAAACCCATCTCTCTGCGGTTT ACATGTATGGATTGATTACTACGCCCGATCGAATCCATATGTAGTTACTCCAAATCATGAGGTAAACAGCAGTTCCGCTAGAAAATGATAAT GAATTAATTAGAAGTTTTAGGATGTTCAACAGCCAGGCGCACAGTTTGTCGACGAGAAAAAGCAATTGTTGGATGAGATTATGGCTCTTGAC GACGCTGCTCAAAAATTGACCGCCTAGTTATTTTAATTATGCTCAGTTATTCAATTTTGTTGTTAGACTTTTAAAAATTTAATTTAGAACTT TTCACTGTGATTTCATTTTGCTTTCTTTATGTGCA	Y110A7A, 35,061–37,303 nt
ocrl-1	ACTGAAAAATGCGATATGACACCCGTTTGTTTAGAAAAGTTTTAAAAAATGATTTGTAAAGTCTGATAAACCCCCGTAAGAAAATTTTATCCT AAGGCAACATCAGGAGCATAGTCACATATAGTTTGTAGTATAGTTGAGAACATTCCATGCATTTTCTCATCTTGAATATCGTGCCGGAATAA TACAGTTGCCCAAAGTGATAATTGATCTGAAAATTACTAAATTATATTATTCTTCAAATTCAACAACACCTTTCAATTCGTATTTCTGACTA AAGAACTCTCGGAGCATCAGACATATCAATTCGAGAACTGCTTGATTCTGTTTGGGAAGACTTGATCGAACAACGGTCCATAATCTGAAAAT GTATTGATTAGAACAATTTTTTTTTTTCAAATAAAATATTACTGTCTGGCATCGGTTCGATATTTTATCATTTCTTTATGAATGATTTTGAAC ATTCCTTCCAAAATTATAGGCTCATCCAGAGAGTCGAGCAATCGTATTAATGCGCTGTACAACATATAAGAAGATGCAAGTTGGCCTGAAAT AAAGAAAATATTAAACAAAATCGTTGATATCCAGAACATGAACATTTCTAGGTAAACATTTTTAGAATTTTCGGTGCTTTTTTTCAAAAAAT CTATTTTTTTATAACAAAAGTGGGCGGAAAAATGAAGAAACAATTCTGTCGATAACTCATAATTTTTTAATTTAATTTTGCACTTTTTCATG CAAAAAATGGCACTCGGAATTGTAGGAATATGCTCAAAATCTTTAACTGTTTCGATTTTTTCCAAACTTGAAAAAAACTTTTCTTTTCCGTT CTCGAAAATAATAAATTCCGGAAACAGTCCCGATTCTTGAAATATTTTTTAAAACTCACTCAAATCGTCGGGCTGTCCAGATTCAAGTGCAG ATCTGATTCTATTAAAGACCTCATTGTCCTGTTCTTCTTCAATATTTAACTGAACTGCTCCACGTGTTCGAAGAGCCATCACAAGCCGATAA ATTACTCGAGGAACATTTGGAGGACAGTTGTCAGAAAGTGAATTTTCCGAGAAATCTCCAAAATCGATGAGATTAACTTCTTTTTTTGGTCT CATTGATAAAAGTTTCTCCAATGTACTTCCAAAGCATGAATTGTTATAAACTGCTGTGATTGGAATAAAATAATCACGTCCATTTTCTAAAT GTAAGACAAGAATTTCTTGGAGCTGCCCATTTCGAATCAAATCTTGAATTCGTCGAACAATATCCGTGCTTATTGATACCGTTAAGCTGATC TGAAATAATCCACTTTTCTCCAGAAAATTATTACCACGAAACAGATCATTAGAGCGAAAACTATTTTAATTGAAGTTTGAATAAAGAAACTT TATACAATAGTGTCCGATGGTTTTTGTCCAGAAAATACATGAAACAGTCTCAATATGCCAAATATAACTGTAAATTATTTTTTCAATTTTTT GAATTCTCGGGCAAATTTGTGAATAAGTTTCGATATTTTTGCGTTTTTCTTCATTTTTAATTACTTTTTATTACATCGAATTTTTCAGGCATTT	C16C2, 2,650–4,215 nt
vps-34	GTTGGATCCCTTTGCATCACGACGTATTGAAATGATCAGAGCTAAATACAAGTACTCATCTCCTGATAGACACGTATTTCTTGTTCTAGAAA TGGCAGCGATTCGATTGGGACCTACTTTTTATAAAGTTGTCTATTATGAAGATGAGACAAAAAATGAAAGGATTTGTTTTTCTACACAGTTT TGGTCTATTTTGAAATCTAACAATTGAGAAACTACAATTTCTGTTTCAAAGAATCAATTATTTTATTCGAAAAGCCTTCCATATTATAATTT TCAACCCAAATTAATTCTACTATGATTTAAAATAACCAAACCAATCAAAAAAAATTTTATCTTGAACTTCGAATTTTCAGATGCGAGTCTCC ACGTCAGTCAACGGTGGTGTTGGGATTGTTTCGGCCTGTACCCGTTACTGTGTAGCTGATCCTGAACTTCTTCTAGAATCTCTGGCGGAAGT TAAACACAGTGCAATGACACGTCGAATCAGAGATGTTGAAGATGAGAGACATCGACAAGTAAAACCGAATAAACAAGCAAAGGATCGATTGG AGACTATTGTGAATCTTCCATCATCTCAAGTTCTTACAAGAGAACAAAGAGATTTAGTATGGAAATTCAGGCATTATTTAAGACAATTTCCA AAAGCTTTGAACAAATATCTACGATCAGTTAATTGGGTTCATCCACAAGAAGTAAAAACTGCATTAGCTCTGATGAATGATTGGGAGCTGAT TGAAGCTGAAGATGCATTAGAATTACTTTCAAGTGCATTCACTCATCCGGCAGTTCGTGCATATTCTGTATCCCGTCTTCTAGAAGCTGCTT CTCCTGAGCAAGTCCTCCTATATCTTCCACAATTGGTTCAAGCTTTGAAATACGAACAAGGTCAACAACTGCCTGAAGAAGGAAATCCAGTG CCGGTGGTTTCTGAAGAAGAGGGAAAGATCCCATCAGTTGCAACTACGCCAACTGAAGAGCTAGAAGGACGAGATATGACAGTGGTTACGAA GAAAGAGGCTAGAAAGGCGGCTAGTGGAGATTTGGCCACCTTCCTGATTGAGTTAGTTGGGAGATAAATTGTTTTTGTTAATTTCAAAAAGT TCTAGGAAAAAATTTTGAAACAAACATTTTAGATGTTTTACTTTATGAAGTTTGAAAAGAGCAACAATTTTTTTTTTGCAATTTCGGCACATA	B0025, 10,243–11,439 nt

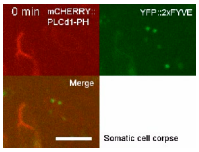

Video 1. **Dynamic changes of PtdIns(4,5)P_2 and PtdIns3P on apoptotic cell–containing phagosomes.** A cell corpse in a wild-type *C. elegans* embryo expressing both mCHERRY::PLCδ1-PH and YFP::2xFYVE is followed. Images were analyzed with a time-lapse confocal microscope using an inverted fluorescence microscope with a spinning-disk confocal scanner unit. The frames were taken every 1 min for 13 min and are displayed every 1 s. Selected images are shown in Fig. 1 A. Bar, 5 µm.

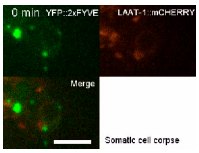

Video 2. **PtdIns3P depletion precedes phagolysosome formation.** A cell corpse in a wild-type *C. elegans* embryo expressing both YFP::2xFYVE and the lysosomal membrane protein LAAT-1::mCHERRY is followed. Images were analyzed with a time-lapse confocal microscope using an inverted fluorescence microscope with a spinning-disk confocal scanner unit. The frames were taken every 1 min for 28 min and are displayed every 1 s. Selected images are shown in Fig. 1 B. Bar, 5 µm.

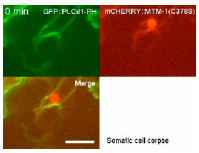

Video 3. **MTM-1 and PtdIns(4,5)P_2 display identical dynamics on extending pseudopods and forming phagosomes.** A cell corpse in a wild-type *C. elegans* embryo expressing both GFP::PLCδ1-PH and mCHERRY::MTM-1(C378S) is followed. Images were analyzed with a time-lapse confocal microscope using an inverted fluorescence microscope with a spinning-disk confocal scanner unit. The frames were taken every 1 min for 8 min and are displayed every 1 s. Selected images are shown in Fig. 1 D. Bar, 5 µm.

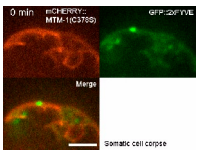

Video 4. **MTM-1 release coincides with PtdIns3P accumulation on phagosomes.** Cell corpses in a wild-type *C. elegans* embryo expressing both mCHERRY::MTM-1(C378S) and GFP::2xFYVE are followed. Images were analyzed with a time-lapse confocal microscope using an inverted fluorescence microscope with a spinning-disk confocal scanner unit. The frames were taken every 1 min for 14 min and are displayed every 1 s. Selected images are shown in Fig. 4 A. Bar, 5 µm.

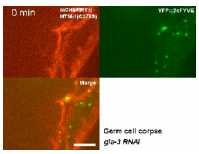

Video 5. **MTM-1 release coincides with PtdIns3P accumulation on phagosomes.** Cell corpses in a *gla-3RNAi* germline expressing both mCHERRY::MTM-1(C378S) and YFP::2xFYVE are followed. Images were analyzed with a time-lapse confocal microscope using an inverted fluorescence microscope with a spinning-disk confocal scanner unit. The frames were taken every 2 min for 60 min and are displayed every 1 s. Selected images are shown in Fig. 4 F. Bar, 5 µm.

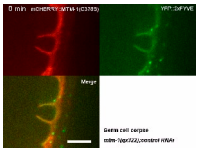

Video 6. **Loss of MTM-1 causes PtdIns3P accumulation on extending pseudopods and forming phagosomes.** The internalization of a germ cell corpse in an *mtm-1(qx322);controlRNAi* animal expressing both mCHERRY::MTM-1(C378S) and YFP::2xFYVE is followed. 2xFYVE appears on the extending pseudopod and nascent phagosome positive for MTM-1(C378S). Images were analyzed with a time-lapse confocal microscope using an inverted fluorescence microscope with a spinning-disk confocal scanner unit. The frames were taken every 2 min for 60 min and are displayed every 1 s. Selected images are shown in Fig. 5 H. Bar, 5 µm.

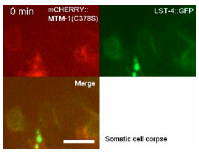

Video 7. **LST-4 and MTM-1 display identical phagosomal dynamics.** A cell corpse in a wild-type *C. elegans* embryo expressing both LST-4::GFP and mCHERRY::MTM-1(C378S) is followed. LST-4 and MTM-1(C378S) appear simultaneously on the extending pseudopod and nascent phagosome and disappear together from the phagosome. Images were analyzed with a time-lapse confocal microscope using an inverted fluorescence microscope with a spinning-disk confocal scanner unit. The frames were taken every 1 min for 15 min and are displayed every 1 s. Selected images are shown in Fig. 6 A. Bar, 5 µm.

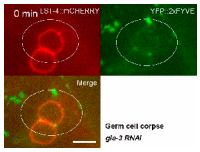

Video 8. **LST-4 release coincides with PtdIns3P accumulation on phagosomes.** A germ cell corpse in a *gla-3RNAi* animal expressing both LST-4::mCHERRY and YFP::2xFYVE is followed. LST-4 release coincides with 2xFYVE enrichment on the phagosome. Images were analyzed with a time-lapse confocal microscope using an inverted fluorescence microscope with a spinning-disk confocal scanner unit. The frames were taken every 2 min for 38 min and are displayed every 1 s. Selected images are shown in Fig. 6 B. Bar, 5 µm.

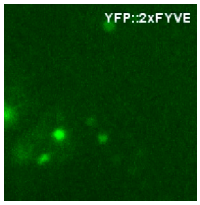

Video 9. **MTM-1 release coincides with PtdIns3P accumulation on the C3 phagosome.** A C3 corpse in a wild-type *C. elegans* embryo expressing both mCHERRY::MTM-1(C378S) and YFP::2xFYVE is followed. MTM-1(C378) disappearance coincides with 2xFYVE enrichment on the C3 phagosome, and no reappearance of MTM-1 is observed. Images were analyzed with a time-lapse confocal microscope using an inverted fluorescence microscope with a spinning-disk confocal scanner unit. The frames were taken every 1 min for 30 min and are displayed every 1 s. Selected images are shown in Fig. S5 H. Bar, 5 µm.